by M. J. Stanich

Print-quality enhancement in electrophotographic printers

Print-quality enhancement (PQE) is a sophisticated form of image enhancement that is used to improve print quality. The benefits of PQE include reduced edge raggedness. control over boldness, stroke-imbalance correction, and improvements to the appearance of patterns that are difficult to print. Use of PQE permits one to obtain highquality printing while using printers with lower resolution than would be required otherwise. Data bandwidth and storage requirements are therefore reduced. PQE relies on an imaging system with multiple exposure levels. A PQE algorithm generates an exposure value for each picture element (pel) based on neighboring bilevel pels. Since the exposure value is generated algorithmically, there is no need to store or internally transmit multiple bits per pel. This paper describes the capabilities of PQE and illustrates the level of print-quality improvements that can be obtained. Imaging-system requirements are presented, with attention to the modulator technology. The major focus is a PQE model that includes the PQE algorithm from the bitmap algorithm through the image-writing process.

Introduction

IBM has used resolution-enhancement technology (using algorithms and modulation techniques to create the

illusion of high-resolution printing on printers with lower resolution than would otherwise be required) in many of its printers since the introduction of the IBM 3820 printer [1] in 1985. In this printer, the technology was primarily used to perform antialiasing—improving the appearance of printed text and graphics by smoothing the steps that would otherwise appear in diagonal lines. With antialiasing, pels that would otherwise look like a step along the edge of a diagonal line are printed at partial exposure levels in order to smooth out the step. Over time, IBM has advanced the technology to also include print-boldness control, stroke-imbalance correction, and improvements to the appearance of patterns that are difficult to print. IBM's enhancement technology is called Print Quality Enhancement (PQE) [1–4].

The print-quality improvement resulting from PQE is achieved by precisely exposing each pel according to the binary pel data surrounding it. The exposure for each pel is established in real time, as the printer operates, by comparing the bit pattern surrounding the pel to be printed to a set of stored patterns. These patterns identify the type of data that can be improved by partial pel exposures. In addition to improving the appearance of diagonal lines and curves, PQE improves other aspects of print quality by controlling boldness and improving the printing of thin lines and isolated dots. Boldness control essentially prints pels along the periphery of an image at reduced exposure levels. The result is reduced width of printed images. Controlling the exposure level of these peripheral pels permits precise balancing of stroke width in the print (process) direction and in the direction

Copyright 1997 by International Business Machines Corporation. Copying in printed form for private use is permitted without payment of royalty provided that (1) each reproduction is done without alteration and (2) the Journal reference and IBM copyright notice are included on the first page. The title and abstract, but no other portions, of this paper may be copied or distributed royalty free without further permission by computer-based and other information-service systems. Permission to republish any other portion of this paper must be obtained from the Editor.

0018-8646/97/\$5.00 © 1997 IBM

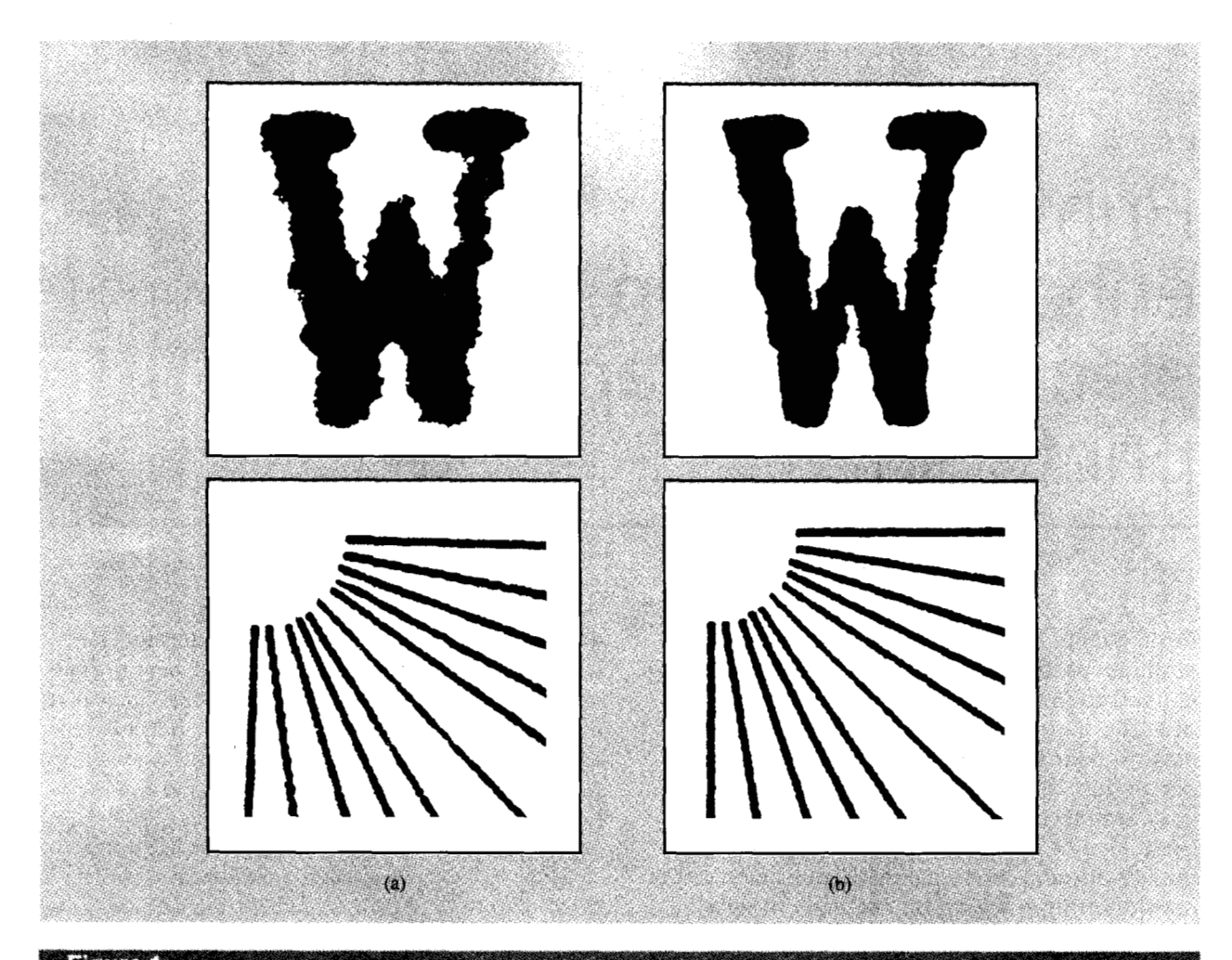


Figure 1

Illustration of improved appearance of "stairstepping" because of PQE: (a) No enhancement (binary mode); (b) enhanced.

perpendicular to the print direction (scan direction). These additional PQE capabilities result in higher image fidelity, which permits printing of high-quality halftone images, line-art graphics, and Kanji characters.

Electrophotographic printers that do not provide quality enhancement print in a binary mode, turning on or off a light-emitting diode or a scanning laser beam for each pel. An example of the output from a printer operating in the binary mode compared to the same printer with PQE is shown in Figure 1. Note the improved smoothness of the edges of the diagonal lines. This illustrates the PQE antialiasing ability. Improvements to the appearance of difficult-to-print characters are shown in Figure 2. Note the better print quality, with reduced "fill-in," for the small text and Kanji character.

Currently, IBM is following a development strategy by which the printer is acquired from original equipment

manufacturer (OEM) vendors. These OEM printer engines are integrated with IBM printer control units and IBM print-enhancement technology. This paper addresses the implementation of PQE in this environment of high-speed printers.

The remainder of this paper describes how PQE was recently implemented in a high-speed, continuous-forms laser printer. Implementation details are reviewed, trade-offs are discussed, and a model used to simulate PQE is presented.

Background

Various antialiasing methods are now common in the printing industry. Two of the best-known implementations are Resolution Enhancement Technology from Hewlett-Packard [5] and Print Quality Enhancement Technology by Lexmark [6]. By comparison to antialiasing in the

670

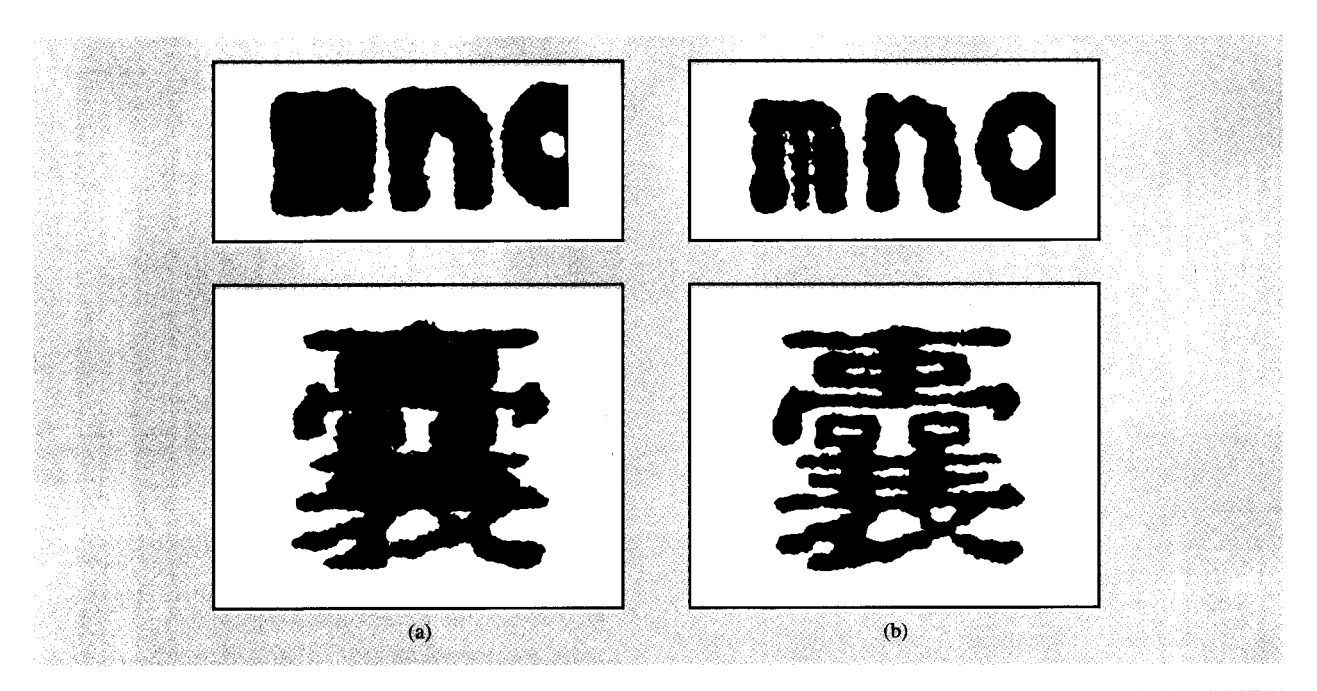


Figure 2

Illustration of improved appearance of small text (6 pt) and Kanji character because of PQE: (a) No enhancement; (b) enhanced.

IBM 3820 printer, today's PQE is a very sophisticated implementation, providing antialiasing and boldness control, and improving the quality of difficult-to-print pel patterns. PQE has been used in laser printers employing semiconductor lasers and gas-laser/acousto-optic modulators (AOMs).

Much has been published on the subject of establishing the optimal parameters for the printheads of laser beam printers [7–9]; however, these papers presented simple models of the image-writing process. The current paper presents a detailed image-writing model that includes partial pel exposures.

Late in 1990, a project was started in the IBM Tucson, Arizona, printer development laboratory to add PQE to the IBM 3835 and 3900 continuous-forms printers. This was a major challenge because of the very high printer speeds and because the printers were not capable of multiple exposure levels (88 and 229 8.5-inch-wide pages per minute, respectively).

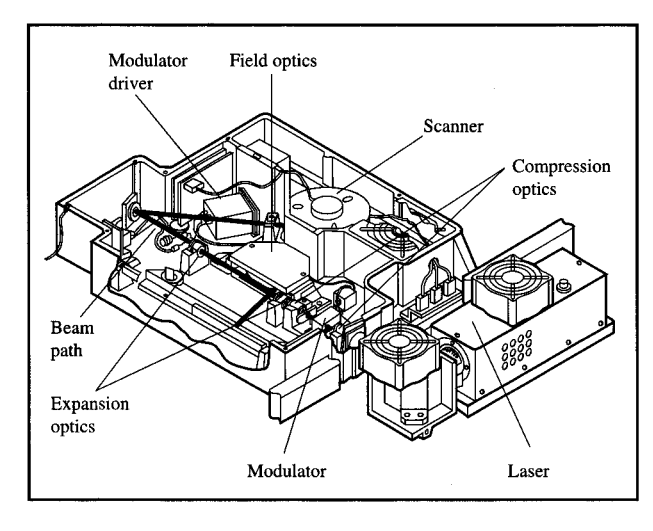
The speed challenge was met by the development of a novel PQE electronic architecture that used high-speed parallel logic, precision clocking, and very accurate synchronization of the modulation data with the scanning of the laser beam. The lack of amplitude modulation was addressed by replacing the existing digital data path to the printhead with an analog path. The existing modulator drivers and modulators were maintained.

Initial feasibility was demonstrated in January 1991, and production implementations followed. PQE was standard on the 3835 and 3900 printers when they were generally available in 1993. When introduced, they were the fastest printers in the industry to feature PQE. PQE has since been implemented on even faster, higher-resolution multiple-laser-beam IBM printers. These include a two-beam printer operating at 310 pages per minute at 240 dots per inch (dpi) and a four-beam, 600-dpi, duplex printing system operating at 150 pages per minute.

We believe PQE improves quality such that a 240-dpi printer with PQE is perceived to be as good as a 300-dpi printer without PQE [1]. Claims have been made that for most text, 300-dpi text with enhancement technology appears as good as if not better than 600-dpi [6].

• Printhead

Figure 3 shows an example of a typical laser printhead for an electrophotographic printer. This particular printhead is used in the IBM 3900 printer. The printhead uses a scanning focused laser beam to write information onto a photoconductor-coated drum. The printhead modifies the beam from the laser, modulating, focusing, and scanning it across the photoconductor by means of an assortment of mechanical, optical, and acousto-optical devices. The basic printhead components are the laser, compression optics, the modulator, the modulator driver, expansion optics, the



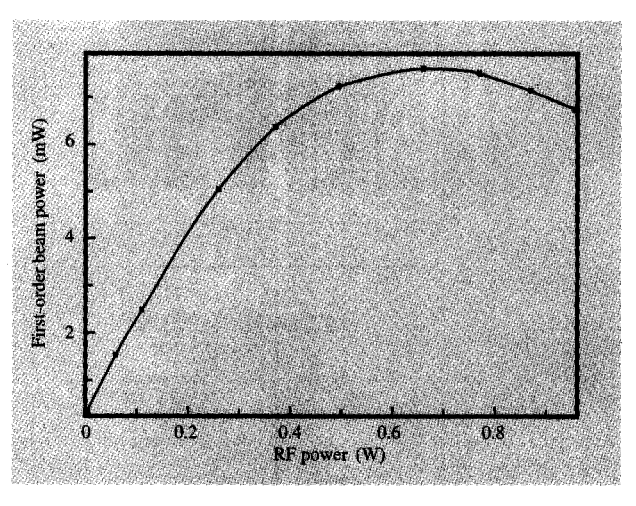


Figure 3

Typical laser printhead. The beam path is shown in red.

Figure 5

Diffracted (first-order) laser-beam power vs. RF power input to AOM piezoelectric transducer.

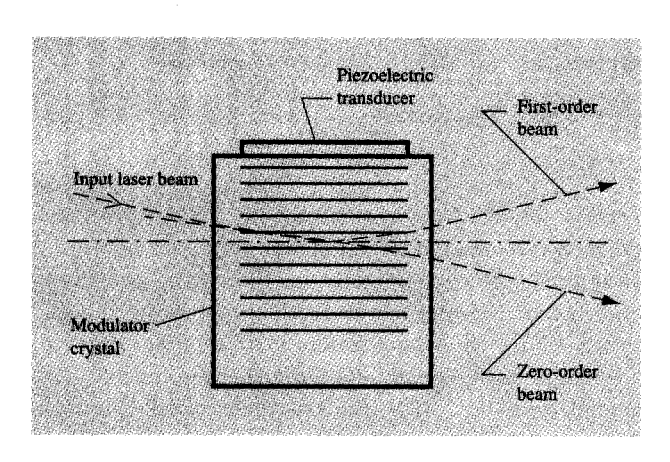


Figure 4 Acousto-optic-modulator beam geometry.

beam is modulated to form each pel. The photoconductorcoated drum advances to the next row of pels every scan, allowing a complete image to be constructed in a typical raster-scan fashion. The example printhead exposes one pel every 27 ns; this is called the pel time.

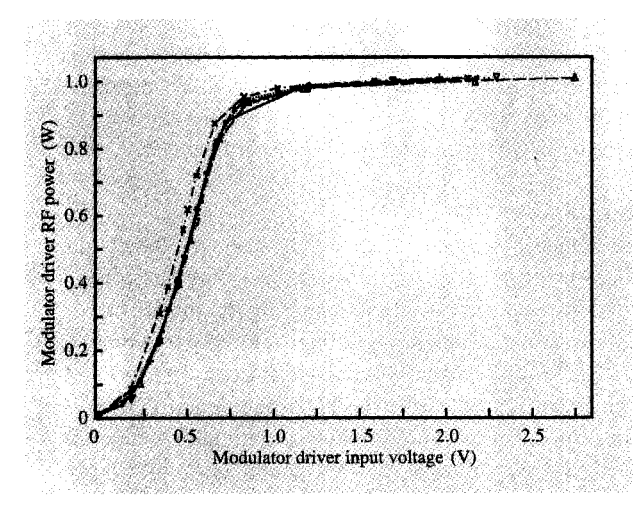
Thus, the optical image, written by the printhead, becomes an electrostatic image as charge moves through the photoconductor. The electrostatic image is "toned" with fine black powder by a "developer." The toned image is transferred to paper and fused by heat and pressure to form a permanent image.

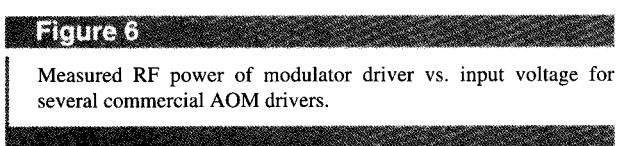
Gas laser printheads require external modulating devices. Semiconductor laser printheads are capable of direct modulation of the laser beam power by altering the drive current to the laser diode. For gas laser printheads like that shown, the acousto-optic modulator (AOM) is a key component for PQE. Its function is to convert the electrical signal from the control unit to a corresponding modulation of the scanning laser beam. The AOM uses a modulation technology employing interaction of sound and light [10, 11].

The AOM consists of a crystal made from a material with photoelastic properties. Such materials change their index of refraction when stressed mechanically. A piezoelectric transducer, which converts electrical signals to stress, is bonded to a face of the crystal. A single-frequency RF signal is applied to the piezoelectric transducer, generating a sound field inside the crystal. This field propagates at the speed of sound through the crystal. Because of the photoelastic property, the propagating field within the crystal causes periodically spaced variations of the index of refraction. This can be

scanner, and field optics. A mirror (not shown) reflects the scanning beam to the photoconductor drum, which is located below the printhead. The printhead shown in Figure 3 employs an argon-ion gas laser as a light source and an acousto-optic modulator for modulating the laser beam power. The printhead of a binary printer without PQE typically turns the beam either fully on or fully off for each pel. PQE requires "partial" pel exposures, which can be produced with either pulse-width modulation or amplitude modulation of the laser beam.

The printhead uses a single scanning laser spot to expose the printer photoconductor. As the writing beam scans across the photoconductor, the power in the laser

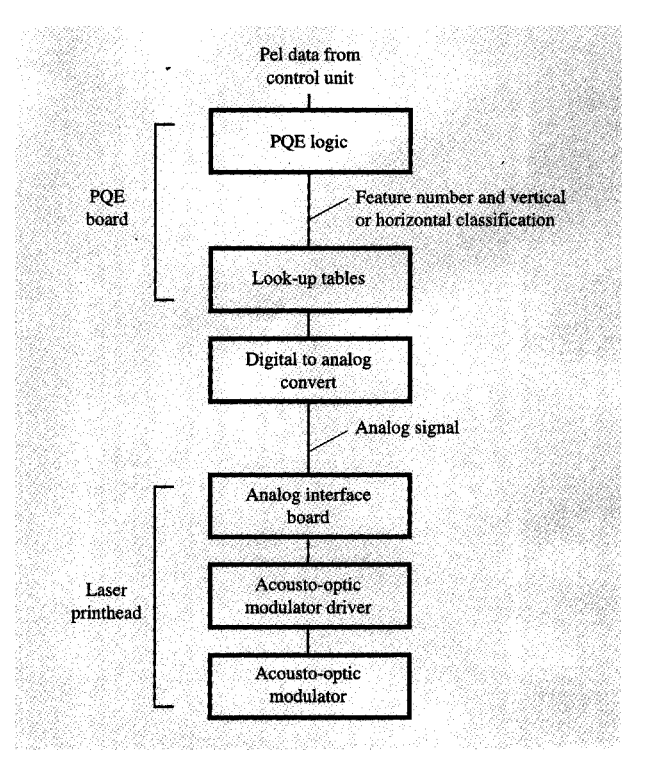




thought of as a moving grating. When the grating is present, a laser beam passing through the modulator crystal is diffracted, essentially splitting into two output beams, called first-order and zero-order. Figure 4 shows the AOM geometry. By controlling the strength of the sound field, one can control the amount of variation of the index of refraction occurring in the moving grating, which controls the relative amount of power in the two beams leaving the modulator. With a suitable driver, beam-power modulation can be accomplished on a pel-by-pel basis.

Within limits, the stronger the sound field, the higher the power that appears in the first-order beam and the lower the power that appears in the zero-order beam. This characteristic is shown in **Figure 5** in the form of a plot of the first-order laser beam power as a function of the input power to the AOM piezoelectric transducer.

Figure 6 shows the measured input/output characteristics of six different modulator drivers. The input/output characteristics of the printhead are a combination of the characteristics of the driver, as shown in Figure 6, and the modulator, Figure 5. The modulator driver has a large linear region, making it possible to modulate the beam to levels from off to full power. Drivers used are high-speed devices capable of modulating laser power on a pel-by-pel basis. Thus, AOMs have amplitude-modulation characteristics suitable for PQE when they are driven by appropriate AOM drivers.





• Amplitude modulation compared with pulse-width modulation The printhead scans a modulated laser beam across the photoconductor drum, writing a raster image on a pel-bypel basis. The field optics focus the laser beam to a small spot, called the writing spot, at the surface of the photoconductor. Decreased pel exposures can be achieved by reducing the power of the writing spot (amplitude modulation) or by decreasing the pel exposure time (pulse-width modulation). In the previous section, the amplitude-modulation capability of the modulator was described. We now touch briefly on pulse-width modulation.

The pel time for the high-speed printer example of Figure 3 is 27 ns. If 32, 64, or 128 different, equally spaced exposure levels are required to implement PQE, pulses as short as 844, 422, or 211 ps, respectively, are required. Achieving these pulse widths and maintaining them reliably is difficult. For this reason, amplitude modulation was selected by IBM as the best choice to implement PQE. The amplitude-modulation approach has now been applied to other higher-speed and higher-resolution IBM printers.

• PQE architecture

Figure 7 shows the organization of the electronics that drive the laser printhead. Pel data from the printer control

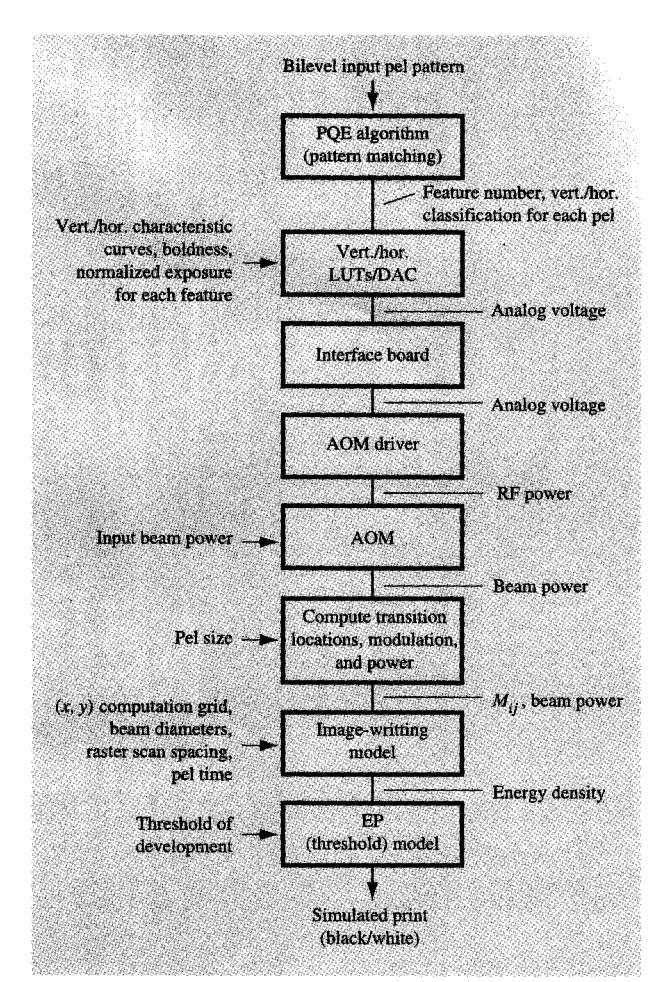


Figure 8
PQE simulation.

unit are passed to the PQE logic, in which the data to be printed are compared with stored pel patterns. In general, a square array of data centered at the current pel to be printed is compared with a set of stored square patterns, resulting in a "feature number" and a classification as "horizontal" or "vertical." A lookup table (LUT) is used to convert the feature number to an exposure value for the current pel being printed. There are two LUTs, one for all the features classified as vertical and one for horizontal. The LUTs are mathematically derived from a characteristic curve for the printer, normalized exposure values for each feature, and a programmable boldness value. The characteristic curve defines the relationship between printed stroke width and required exposure power. The two tables allow correction for printed strokewidth differences between the "vertical" and "horizontal" directions (stroke-width imbalance).

The exposure value is sent to a digital-to-analog converter (DAC), which produces an amplitude-modulated signal that is fed to the printhead through an interface board. The signal controls the modulator driver and, through it, the modulation of the laser beam.

Simulating PQ

Although the development of PQE has been largely done empirically, through subjective print-quality tests, modeling can play a role in analyzing the effects of different enhancement algorithms (stored pel patterns), LUTs, spot sizes, and modulation devices. The focus of this paper is to describe the PQE system and PQE modeling. This section develops a method of simulating PQE using a model of the PQE architecture previously described, combined with a scanning-spot-image-writing model

Figure 8 is a block diagram of the PQE simulation. The simulation variables are shown on the block diagram and include beam power, spot sizes (vertical and horizontal), POE algorithm, LUTs, boldness, characteristic curves, pel time, and grid points. (Boldness relates to peripheral-pel exposure levels.) The electrical transfer functions for the AOM, AOM driver, and interface board are included in the simulation as well as the image-writing model, which yields results in terms of energy density of the image written on the photoconductor. This is converted to the simulated printed image by a "threshold of development" (energy density of the transition point from black to white grid points) model of the electrophotographic (EP) process. (The model could be improved by using a more sophisticated model of the EP process [12, 13]. Without this improvement, the simulation still provides useful results that furnish valuable insight into the workings of a complex system.) Artifacts caused by the PQE algorithm can quickly be analyzed by use of the model and their source understood. Figure 9 illustrates images obtained by simulation together with actual print samples. The figure shows how closely the simulated results correspond to the actual results, the major difference being due to the noise from the EP process.

The focused spot at the photoconductor surface for a laser printhead has a Gaussian profile because the laser beam from the gas laser, used as a light source, has a TEM_{00} mode (Gaussian). The size of the laser profile is changed by the focusing action of the lenses; however, the shape remains the same. A Gaussian spot profile is shown in **Figure 10**. The writing spot formed by a semiconductor laser also can be approximated with a Gaussian spot. Spots are typically designed to be elliptical (narrower in the direction of scanning) in order to compensate for the convolution spreading that occurs because of the scanning motion of the spot while the beam is modulated.

To obtain a practical numerical solution to the image-writing model, we assume a one-dimensional spot profile for each axis of the exposure spot. The two-dimensional profile is assumed to be the product of the two profiles. Data experimentally obtained from two orthogonal scanning-slit spot-profile measurements are used to determine the two profiles [14]. The measurements involve scanning a long, narrow slit past a stationary laser beam in the scan and process directions, while collecting data on transmitted power vs. position. One obtains the beam profile sizes by fitting the profile data to a Gaussian curve. Other methods can be employed to measure spot profile, including analyzing images from CCD cameras or data from knife-edge scans.

• Mathematical basis

In this section, the mathematical basis for the simulation model is developed. Starting with the writing-spot profile and adding the motion of the writing spot and modulation of the spot power, we obtain a general expression for the two-dimensional energy density. Simplifying assumptions are applied to the general expression, and results are obtained for a Gaussian spot profile. The equations are finally extended to multiple scan-line images with multiple beam-power transitions.

The model assumes a stationary medium exposed by a linearly translating, amplitude-modulated writing spot. The energy density at any point is determined by adding the contributions from all raster scan lines.

Assume that function A(x, y) represents the twodimensional, normalized (to unity) spot profile. The spot irradiance distribution (exposure spot profile function) Ecan then be expressed as E(x, y) = E'A(x, y) where E' is a constant proportional to the total power P contained in the spot (irradiance has units of power per unit area):

$$E' = \frac{P}{\int_{-\infty}^{\infty} \int_{-\infty}^{\infty} A(x, y) \, dx \, dy}$$
 (1)

The irradiance distribution (spot) is now assumed to be moving in the y direction at a velocity given by the function V(Y), where Y is the y-direction position of the center of the irradiance distribution. The power of the spot changes as the spot moves and is given by the normalized (to unity) modulation function M(Y). The total spot power is PM(Y). If the modulation of the spot is ignored, the irradiance E at any point x, y is E'A(x, y - Y). The incremental energy density (D) at point x, y is the product of the irradiance E(x, y - Y), the modulation M(Y), and the incremental exposure time dt.

$$dD(x, y - Y) = E'A(x, y - Y)M(Y) dt.$$
 (2)

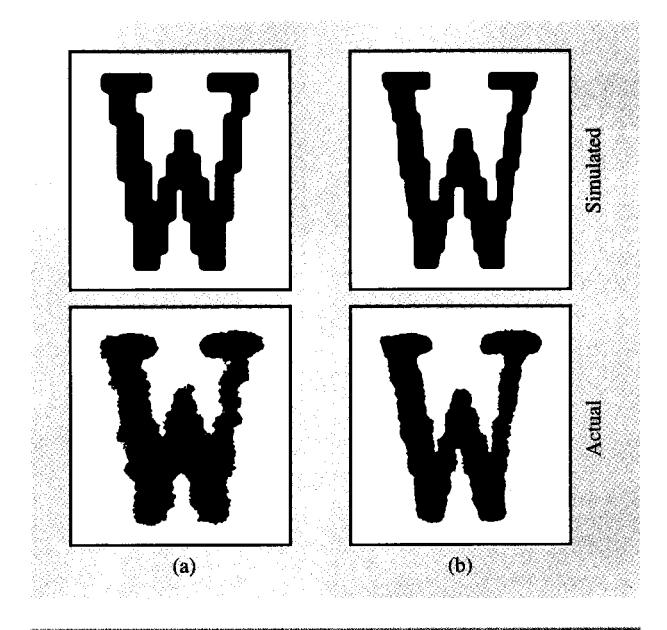


Figure 9

Simulated results and actual results, (a) without PQE and (b) with PQE. Actual results are taken from Figure 1.

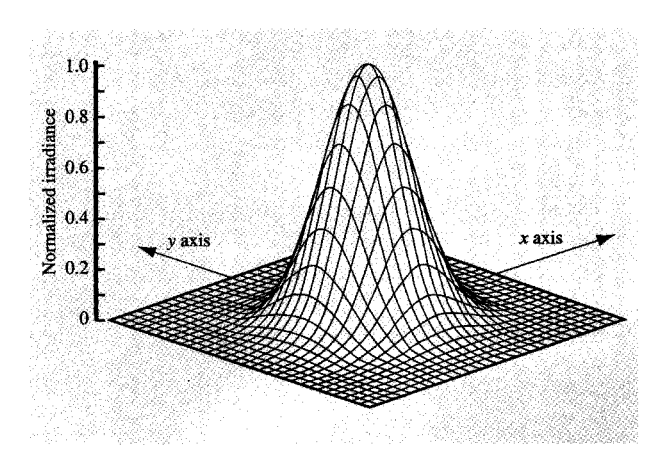


Figure 10

Gaussian spot profile function A(x, y).

Since the velocity of the spot motion $V(Y) \equiv dY/dt$, we can write

$$dD(x, y - Y) = \frac{E'A(x, y - Y)M(Y)}{V(Y)}dY.$$
 (3)

Integrating Equation (3), we obtain a general expression for the energy density:

675

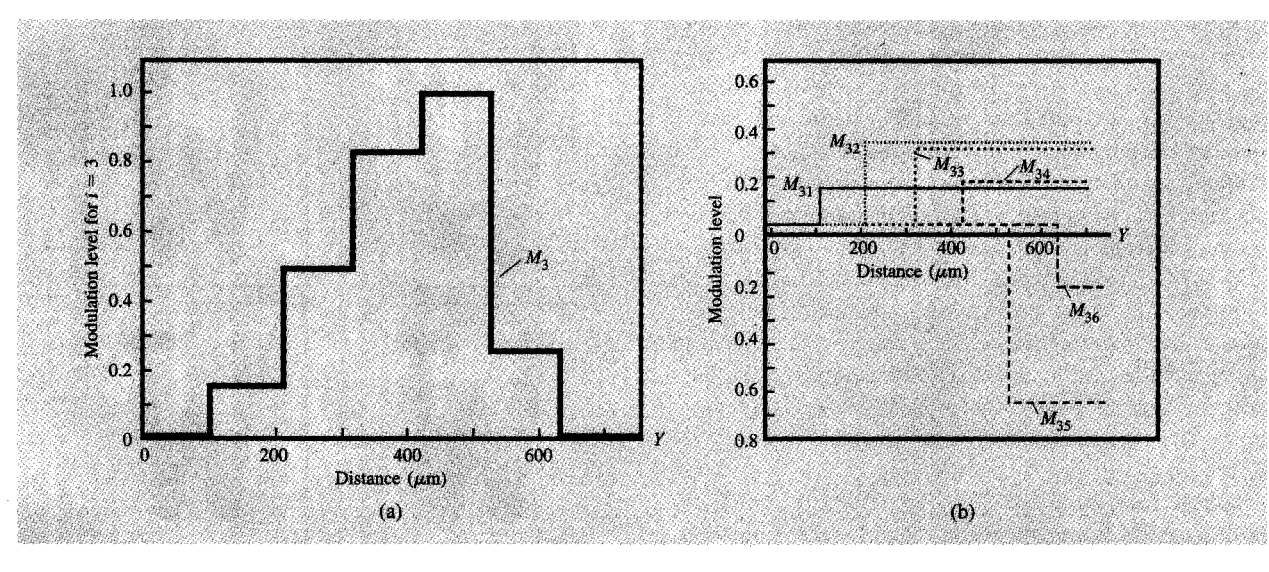


Figure 11

(a) A modulation function; (b) its component step functions

$$D(x,y) = E' \int_{-x}^{\infty} \frac{A(x,y-Y)M(Y)}{V(Y)} dY.$$
 (4)

We next apply the simplifying assumptions to the general expression, Equation (4), to obtain an expression that can be quickly solved numerically:

- 1. The spot is moving at constant velocity V.
- 2. The normalized (to unity) spot profile A(x, y) is the product of two profile functions, F(x) and G(y).

With these assumptions, the irradiance is

$$E(x, y) = E'A(x, y) = E'F(x)G(y).$$

The scaling factor E' becomes

$$E' = \frac{P}{\int_{-\infty}^{\infty} F(x) \ dx \int_{-\infty}^{\infty} G(y) \ dy}$$
 (5)

Finally, the energy density is

$$D(x,y) = \frac{E'F(x)}{V} \int_{-\infty}^{\infty} G(y-Y)M(Y) dY.$$
 (6)

Complex images

In this section, we extend the solution for a single scan with the simplifying assumptions, Equation (6), to images

formed by multiple adjacent raster scans, referred to as complex images. A complex image might be the exposure required to print a character or a halftone pattern.

The solution for a complex image is obtained by summing, at each point, the energy density contribution from each scan. The energy density for a complex image is

$$D(x,y) = \sum_{i=1}^{n} \frac{E_{i}' F_{i}(x-p_{i})}{V_{i}} \int_{-\infty}^{\infty} G_{i}(y-Y) M_{i}(Y) dY, \qquad (7)$$

where p_i is the x-axis location of scan i, n is the total number of exposure scans, and V_i , M_i , E_i , F_i , and G_i are corresponding constants and functions for the ith scan.

We now make the following additional assumptions:

- 1. Profile functions F(x) and G(y) are constant for all exposure scans.
- 2. Spot power *P* is constant.
- 3. Spot velocity V is constant.

Consequently, E' is constant, and

$$D(x, y) = \sum_{i=1}^{n} \frac{E'F(x - p_i)}{V} \int_{-\infty}^{\infty} G(y - Y) M_i(Y) dY.$$
 (8)

The integral in Equation (8) is the convolution $M_i * G$ of the modulation function M_i and the profile function G.

An additional simplification is added by assuming that the modulation function M_i steps between discrete levels. An example of this is shown in Figure 11 for one raster

676

scan. We express the modulation function as a summation of single-step functions $M_{ij}(Y)$, where m_i is the number of transitions for scan i. The value m_i will vary from zero, for a scan in which the beam is never turned on, to the maximum number of transitions for all scans for the most "complex" raster scan. Figure 11(b) shows the step functions $M_{ij}(Y)$ corresponding to the modulation function of Figure 11(a). Thus,

$$M_i(Y) = \sum_{i=1}^{m_i} M_{ij}(Y).$$

The convolution of the modulation and y-direction profile functions becomes

$$M_i * G = \left(\sum_{j=1}^{m_i} M_{ij}\right) * G.$$

Applying the distributive property of convolution, we obtain

$$M_i * G = \sum_{i=1}^{m_i} (M_{ij} * G).$$

This expression states that the convolution of the modulation function with G is equivalent to the summation of a set of convolutions, each of which is a single-step transition convolved with G. Applying this result to Equation (8), we determine the energy density:

$$D(x,y) = \sum_{i=1}^{n} \frac{E'F(x-p_i)}{V} \sum_{j=1}^{m_i} (M_{ij}^*G).$$
 (9)

Equation (9) has a simple interpretation: For a single raster scan, the energy density is proportional to the summation of a set of line-spread functions [the one-dimensional functions resulting from convolving G(y) with a single-step transition at y=0] for the y-direction profile that have been scaled and translated to the location of each modulation transition. In the x direction, the energy density is proportional to the x-direction spot profile. Summing the result for all raster scans results in the total energy density.

Profile functions F(x) and G(x)

The TEM_{00} -mode laser-spot profiles can be accurately modeled by the Gaussian function, a bell-shaped curve. This is the most common profile produced by gas lasers. The Gaussian function has a single parameter: the beam radius

The following derivation can be used to compute Equation (9) when F and G are Gaussian functions. For the x-direction profile,

$$F(x) = e^{-2x^2/a^2}$$

where 2a is the $1/e^2$ diameter [width between the two points (x = a and -a) where the irradiance is 13.5% of the maximum irradiance] of the x-direction Gaussian profile, and

$$\int_{-\infty}^{\infty} F(x) \ dx = a \sqrt{\pi/2}.$$

Similarly, for the y-direction,

$$G(y) = e^{-2y^2/b^2},$$

where 2b is the $1/e^2$ diameter of the y-direction Gaussian profile, and

$$\int_{-\infty}^{\infty} G(y) \ dy = b \sqrt{\pi/2}.$$

For a Gaussian profile, the spread function corresponding to a single power transition (at y = 0), which is scaled and summed to form the solution given in Equation (9), does not have a closed-form solution. It can be accurately approximated, however, by error-function approximation algorithms such as [15].

Other profile functions

Non-Gaussian writing-spot profiles, for example the arctangent function used by Williams [16], are useful to simulate other printhead technologies such as LED (light-emitting-diode) arrays. The result is a closed-form solution that does not require approximating algorithms. To model LED printheads, the same mathematics that has been presented applies, except that a ninety-degree rotation of the frame of reference is required. This is because the exposure spots from an LED array are stationary; therefore, modulation occurs in the process direction.

Concluding remarks

This paper has described how acousto-optic-modulator technology in a laser printhead is used to modulate a laser beam at the varying power levels required for PQE. Some of the fundamental implementation decisions were discussed, and the architecture for a printer with PQE was described. Finally, modeling the effects of printing using partial pel exposures was presented, and it was demonstrated how simulated results approximate the actual print quality.

We observe that PQE provides significant print-quality improvements without the need for higher-resolution printing. Furthermore, in traditional electrophotographic printers without PQE, boldness of printing is fixed and cannot be varied without changing the printer set-points,

whereas in printers having PQE the boldness of printing can be adjusted independently of the printer set-points (set-points include charge levels and magnetic-brush bias voltages).

In the future, printers will provide significant additional challenges for PQE implementations, with higher speeds, multiple imaging beams, multiple resolutions, higher resolution, and color. While the role of PQE for these future printers will change, PQE will continue to play an important part, providing significant quality improvements. For example, at very high resolution, the requirement for antialiasing decreases because edge raggedness is reduced as smaller pels are used. (The threshold of human vision is reached at about 2400 dpi [5]. These high resolutions and their corresponding data rates are very difficult to achieve for high-speed printers.)

Acknowledgments

The author recognizes Jack L. Crawford as the pioneer of print-quality enhancement within IBM. The author developed the model for simulating PQE described in this paper and was responsible for the changes required to the laser printhead during the feasibility demonstration of PQE in the 3900 and 3835 printers. In addition, the following individuals were involved with implementing PQE on the 3900 and 3835 printers: Stanley Ciminiski, William Bateman, William Bunn, Larry Ernst, Margarita Sobrino, Gregory Weller, Ben West, Paul Wick, Fred Willis, and John Wilson.

References

- 1. S. Kantor, "Print Enhancement for Electrophotographic Laser Printers," *IBM 3820 Page Printer Technology*, IBM Publication No. S544-3083-0, ISBN 0-933186-22-3, pp. 37-42.
- Jack L. Crawford, "Fidelity Control of Electrophotographic Print Process," Proceedings of the SPSE/SPIE Symposium on Electronic Imaging—Hard Copy Output, January 17–20, 1989, pp. 352–360.
- 3. Jack L. Crawford, "Alternatives to High Resolution: Print Quality Enhancement Methods for Electrophotographic Printers," presented at Business Information Strategists 8th Annual Print Quality Seminar, Boston, November 1-3, 1989.
- J. L. Crawford and D. Elzinga, "Improved Print Quality by Recording Power Modulation," Conference Record, Electronic Imaging 88—Institute for Graphic Communication, October 3-6, 1988, pp. 516-522.
- Charles Tung, "Resolution Enhancement Technology in Hewlett-Packard Laser Jet Printers," Proc. SPIE 1912, Color Hard Copy and Graphic Arts II, 440-448 (1993).
- Gary Overall and Phil Wright, "IBM Laser Printer 4029 Series Print Quality Enhancements," *Personal Systems*, pp. 7-12 (January 1992).
- N. Kawamura and M. Itoh, "The Effect of Exposure on Image Reproduction in Laser Beam Printer," J. Imaging Technol. 15, 212-216 (1989).
- 8. Takashi Nishimura and Yasushi Hoshino, "Electrophotographic Color Printing Using Elliptical Laser Beam Scanning Method," *J. Imaging Technol.* 12, 329–333 (1986).

- 9. H. Sonnenberg, "Laser-Scanning Parameters and Latitudes in Laser Xerography," *Appl. Opt.* 21, No. 10, 1745-1751 (1982).
- Richard V. Johnson, "Temporal Response of the Acoustooptic Modulator; Geometric Optics Model in the Low Scattering Efficiency Limit," Appl. Opt. 16, No. 2, 507-514 (February 1977).
- Richard V. Johnson, "Temporal Response of the Acoustooptic Modulator in the High Scattering Efficiency Regime," Appl. Opt. 18, No. 6, 903-907 (March 1979).
- Robert P. Loce, William L. Lama, and Martin S. Maltz, "Modeling Vibration-Induced Halftone Banding in a Xerographic Laser Printer," J. Electron. Imaging 4, No. 11, 48-61 (1995).
- Nancy B. Goodman, "Latitude Determination for a Xerographic Printer via Computer Modeling," J. Imaging Technol. 14, No. 5, 132-135 (October 1988).
- Rick DeMeis, "How to Select a Beam Profiler to Match Your Application," Laser Focus World 31, No. 4, 133-137 (April 1995).
- Milton Abramowitz and Irene A. Stegun, Handbook of Mathematical Functions, National Bureau of Standards, Washington, DC, 1968, ISBN 0-88307-589-X.
- Edgar M. Williams, "Electrostatic Field of Arctangent Voltage Transitions in Electrophotographic Images," Photographic Sci. & Eng. 26, No. 2, 88-91 (March/April 1982).

Received April 17, 1996; accepted for publication July 8, 1996

Mikel J. Stanich IBM Printing Systems Company, 6300 Diagonal Highway, Boulder, Colorado 80301 (mstanich@vnet.ibm.com). Mr. Stanich is an Advisory Engineer in the Continuous Forms Advanced Printer Engineering Department at the Boulder facility, where he joined IBM in 1974 after receiving a B.S. in mechanical engineering from the University of Arizona. He has worked in the areas of print-quality enhancement, print quality, image scanning/processing, and printhead technology. Mr. Stanich received an IPD Division Award in 1982 for printhead technology. He is a first-level inventor and currently holds three patents, and has published three papers on printheads and printhead technology.